Available online at www.sciencedirect.com
ScienceDirect
Journal of Power Sources 179 (2008) 435–440
JOURNAL OF POWER SOURCES
www.elsevier.com/locate/jpowsour

Short communication

Ideal pseudocapacitive performance of the Mn oxide anodized from the nanostructured and amorphous Mn thin film electrodeposited in BMP–NTf_2 ionic liquid

Jeng-Kuei Chang [a,*], Chiung-Hui Huang [a], Wen-Ta Tsai [a], Ming-Jay Deng [b], I.-Wen Sun [b]

[a] *Department of Materials Science and Engineering, National Cheng Kung University, 1 Ta-Hsueh Road, Tainan 701, Taiwan*
[b] *Department of Chemistry, National Cheng Kung University, Tainan, Taiwan*

Received 5 July 2007; received in revised form 17 December 2007; accepted 18 December 2007
Available online 4 January 2008

Abstract

A novel electrochemical route to prepare the Mn oxide with ideal pseudocapacitive performance is successfully proposed in this study. In *n*-butylmethylpyrrolidinium bis(trifluoromethylsulfony)imide (BMP–NTf_2) ionic liquid, a nanostructured and amorphous Mn film could be electrodeposited on a Ni substrate. The metallic Mn films were then anodized in Na_2SO_4 aqueous solution by the potentiostatic, galvanostatic, and cyclic voltammetric methods and transformed to Mn oxides. It was confirmed that the different anodization courses would cause variations in the material characteristics of the prepared Mn oxides and therefore in their pseudocapacitive performance. The Mn oxide anodized by the cyclic voltammetric method showed the most promising specific capacitance of 402 F g^{-1}; moreover, its capacitance retained ratio after 500 charge–discharge cycles was as high as 94%.

Keywords: Supercapacitor; Pseudocapacitance; Mn oxide; Ionic liquid; Nanostructure

1. Introduction

Electrochemical supercapacitors are the charge-storage devices that have a greater power density and longer cycle life than batteries, and they possess a higher energy density as compared with conventional capacitors [1]. The natural abundance and low cost of manganese (Mn) oxide, accompanied by its satisfactory electrochemical performance in mild electrolytes and environmental compatibility, have made it one of the most promising electrode materials for supercapacitors. Owing to the fast and reversible faradic redox reaction of the electroactive Mn oxide, pseudocapacitive behavior of the oxide electrode can be recognized [2–4]. Recently, various kinds of processes, including thermal decomposition [5–6], coprecipitation [2,7,8], sol–gel processes [3,9,10], physical vapor deposition [11], hydrothermal synthesis [12] and anodic deposition [13,14], etc., have been developed to prepare the Mn oxides with demanding electrochemical properties. It was confirmed that the preparation methods and/or conditions could significantly affect the material characteristics of the obtained Mn oxides, and consequently their corresponding pseudocapacitive behavior. The typical specific capacitances of Mn oxides that have been reported in the literature are in the range of 100–300 F g^{-1} except those extremely thin oxide films [3,4]. Undoubtedly, searching for a more suitable fabrication process to prepare the Mn oxide with superior capacitive performance is an issue of great importance and interest.

Since the pseudocapacitance of Mn oxide is associated with the reversible redox reaction between its trivalent and tetravalent forms [3,4,15,16], the theoretic specific capacitance should be above 1100 F g^{-1}. However, both the poor electronic and ionic conductivity of the Mn oxide have kept it from approaching the ideal electrochemical performance [17]. Much research effort has been devoted to optimize the microstructure of the Mn oxide. For example, nanotechnology is adopted to improve the utilization of this electroactive material and so does its specific capacitance. On the other hand, developing a more

* Corresponding author. Tel.: +886 6 2757575x62942; fax: +886 6 2754395.
E-mail address: catalyst@mail.mse.ncku.edu.tw (J.-K. Chang).

0378-7753/$ – see front matter © 2008 Elsevier B.V. All rights reserved.
doi:10.1016/j.jpowsour.2007.12.084

effective and convenient method to prepare the Mn oxide is another notable issue especially from the viewpoint of commercial applications. Since the anodic deposition is able to prepare the Mn oxide electrode by a simple single-step procedure [13,14], this electrochemical process is considered to be one of the most promising candidates. Another important benefit of using the electrochemical preparation process is the ease of controlling the thickness, morphology, porosity, and chemical states of the obtained oxides (by simply adjusting the electroplating parameters). Optimization of pseudocapacitive performance of the anodically deposited Mn oxide was attempted by several approaches in our previous studies [18–21], however, the specific capacitance was not higher than 250 F g^{-1}. In this paper, we would propose another novel electrochemical route to prepare the Mn oxide with much more ideal pseudocapacitive performance. A nanostructured, amorphous, and metallic Mn thin film is cathodically deposited in *n*-butylmethylpyrrolidinium bis(trifluoromethylsulfony)imide (BMP–NTf_2) ionic liquid. After this film being electrochemically transformed to the Mn oxide by a proper anodization condition, the specific capacitance over 400 F g^{-1} can be obtained.

2. Experimental

The BMP–NTf_2 ionic liquid with 0.05 M Mn(II) cations was prepared according to the previous literature [22,23]. Mn thin films were cathodically deposited on nickel (Ni) substrates in the above-mentioned ionic liquid stirred by a magnetic paddle at 50 °C. The deposition process was performed under a purified nitrogen atmosphere in a glove box (Vacuum Atmosphere Co.), in which the moisture and oxygen contents were maintained below 1 ppm. A three-electrode electrochemical cell controlled by an AUTOLAB potentiostat was adopted for this experiment. The Ni foil (with the exposed area of 1 cm^2 and the thickness of 120 μm) was etched in 1 M H_2SO_4 solution at 85 °C, then washed with pure water in an ultrasonic bath, and finally used as the working electrode after drying. The reference electrode was a Pt wire placed in a fritted glass tube containing BMP–NTf_2 ionic liquid with the ferrocene/ferrocenium couple (Fc/Fc^+, +0.55 V vs. SHE) as the internal reference standard. In addition, the counter electrode was a Mn block which can compensate the consumption of Mn cations in the ionic liquid. During the electrodeposition process, a cathodic potential of −1.8 V (vs. Fc/Fc^+ couple) was applied to yield a total passed charge of 0.3 C cm^2. The obtained Mn films were thoroughly cleaned with CH_2Cl_2 solution and then dried in air. To prepare the Mn oxides, the metallic Mn films were anodized in 0.1 M Na_2SO_4 aqueous solution at 25 °C. In this experiment, a saturated calomel electrode (SCE) and a platinum sheet were used as the reference and counter electrodes, respectively. There were three different anodization courses performed in this study; they included (1) Potentiostatic method: a constant potential of 0.9 V was applied for 10 min. The corresponding anodic current density would rapidly decay from approximately 15 mA cm^2 to a steady value less than 0.1 mA cm^2 after 100 s. The prepared oxide electrode is denoted as Mn oxide–P. (2) Galvanostatic method: a constant current density of 0.3 mA cm^2 was applied while the electrode potential gradually increased from around 0 V to a cutoff point of 0.9 V. The prepared oxide electrode is denoted as Mn oxide–G. (3) Cyclic voltammetric method: a potential sweep rate of 25 mV s^{-1} was performed within a range of 0–0.9 V. It was repeated for 10 cycles because no further irreversible anodic reaction could take place afterward. The prepared oxide electrode is denoted as Mn oxide–CV. All the total anodic charges of the three methods were approximately 0.1 C cm^2, and further oxidation was quite difficult to execute. The obtained Mn oxides were totally dissolved in 2 M HNO_3 solution and the amounts of Mn were quantified by an atomic absorption spectroscope (AAS, SOLAAR M6). Accordingly, the weight of the oxide could be evaluated by referring to its chemical composition (Mn/O ratio). The typical oxide loading weight on the substrate was approximately 0.1 mg.

The morphology and chemical composition of the samples were examined with a scanning electron microscope (SEM, Philip XL-40FEG) and its auxiliary X-ray energy dispersive spectroscope (EDS). Glancing angle X-ray diffraction (GAXRD) analyses were also performed with a Rigaku D/MAX 2500 diffractometer to explore the crystal structure. An X-ray photoelectron spectroscope (XPS, VG ESCALAB 210) was used to inspect the chemical states of the different oxides. Aluminum Kα (1486.6 eV) radiation was utilized as the X-ray source; and the pressure in the analyzing chamber was approximately 1×10^{-9} Torr. In addition, the electrochemical behavior of the various Mn oxides was studied by cyclic voltammetry (CV) in 0.1 M Na_2SO_4 solution at 25 °C. The adopted potential scan rate was in a range of 5–150 mV s^{-1}. Moreover, electrochemical stability of the oxide electrodes was evaluated by repeating the CV test for 500 cycles. The decay in the specific capacitance versus the cycle number was recorded.

3. Results and discussion

Fig. 1 shows the schematic diagram of the electrodeposition of Mn in BMP–NTf_2 ionic liquid. It was found that the Mn cation can be reduced to its metallic state on the Ni substrate at a sufficiently negative potential, beginning at −1.75 V (vs. the Fc/Fc^+ reference). Meanwhile, the dissolved Mn cations from the counter electrode can compensate their consumption during the deposition process. Both the weight gain of the working electrode and the weight loss of the counter electrode were measured with a microbalance after passing a given amount of charge. The experimental data confirmed that the conversion efficiency was above 95%. In addition, the Mn cations in the ionic liquid were already known to be divalent in our previous study [23]. With these understandings, it would be truly easy to electrodeposit a Mn thin film with desired thickness in the ionic liquid. In addition, the obtained Mn films were found to be continuous and adhesive on the Ni substrate. A convenient and effective process to prepare a Mn thin film was thereby proposed.

Fig. 2(a) shows the surface morphology of the as-deposited Mn film examined by the SEM, revealing that it is composed of numerous spherical nanoparticles with the diameter of approximately 50 nm. Fig. 2(b) exhibits the SEM micrograph of the Mn oxide–P electrode. As compared with Fig. 2(a), it is found that

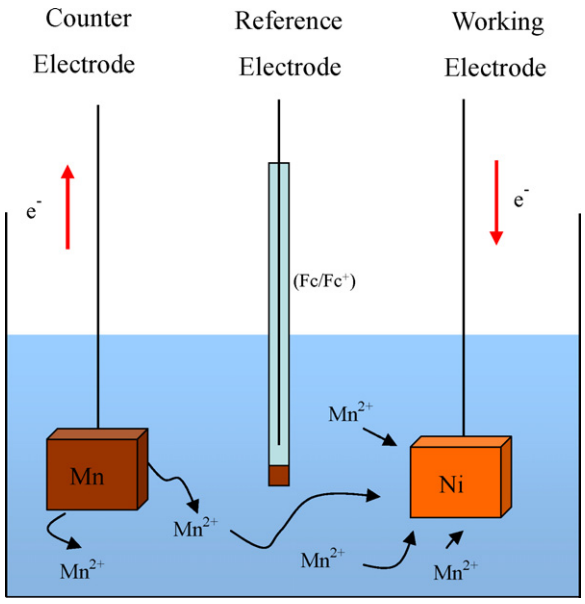

Fig. 1. The schematic of Mn electrodeposition in BMP–NTf_2 ionic liquid.

the as-deposited Mn nanoparticles would lump together after being oxidized because of their volume expansion. Furthermore, since a high constant potential (−0.9 V vs. SCE) was applied and the electrode was rapidly passivated during the anodization process, the formed oxide was rather compact. As shown in Fig. 2(c), the morphology of the Mn oxide prepared by the galvanostatic condition is different from that of the Mn oxide–P electrode. In addition to the compact oxide blocks, some finely whiskery structure is also found. Fig. 2(d) demonstrates the unique microstructure of the Mn oxide–CV electrode. Because the applied potential was swept back and forth to anodize the film, the obtained oxide was highly porous and showed a clearly nano-fibrous morphology on its surface. These SEM observation results indicate that the different anodization courses could indeed cause the change in the oxide morphology. The chemical compositions of the three prepared Mn oxides were examined by the EDS. The analytic data revealed that no impurity (besides Mn and O) was contained in the oxides. Moreover, the Mn/O atomic ratios for the Mn oxide–P, Mn oxide–G, and Mn oxide–CV were 38/62, 41/59, and 43/57, respectively. Fig. 3 shows the GAXRD patterns of the as-deposited Mn and the Mn oxide–P electrodes; actually, the Mn oxide–G and Mn oxide–CV electrodes reveal the similar analytical results. The only diffraction peaks detected are associated with the Ni substrates; no signal from the deposits can be found. These experimental data suggest that the deposited Mn and the Mn oxides are amorphous in nature, whose characteristic is considered to be beneficial for their pseudocapacitive performance.

Fig. 4(a) shows the Mn $2p_{3/2}$ orbit XPS spectra of the three oxides. As demonstrated, a clear peak shift in binding energy due to the different anodization conditions can be recognized. The Mn oxide–P, Mn oxide–G, and Mn oxide–CV samples show their peak positions at 642.5 eV, 642.3 eV, and 642.1 eV, respectively. It was reported in the literature [24,25] that the binding energies of the Mn $2p_{3/2}$ electron increased with its valent state, advancing from 641.6 eV for Mn_2O_3 to 642.6 eV for MnO_2. The comparison results indicated that in all the prepared oxides, the Mn was present in both trivalent and tetravalent states. Moreover,

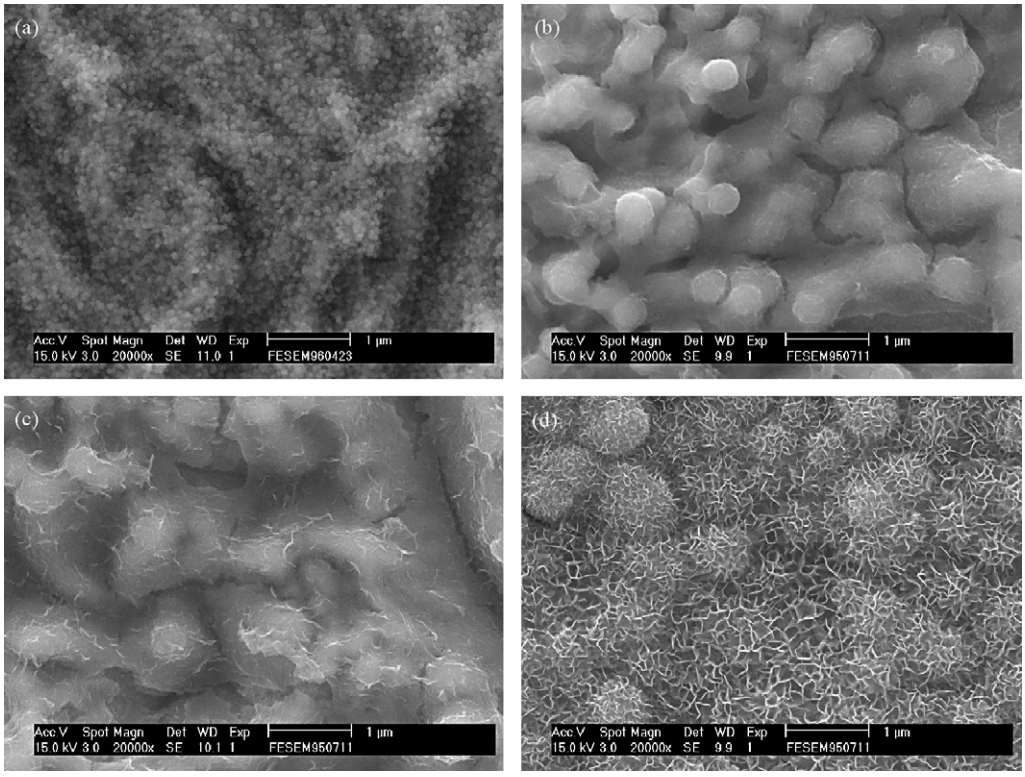

Fig. 2. SEM micrographs of the (a) as-deposited Mn, (b) Mn oxide–P, (c) Mn oxide–G, and (d) Mn oxide–CV electrodes.

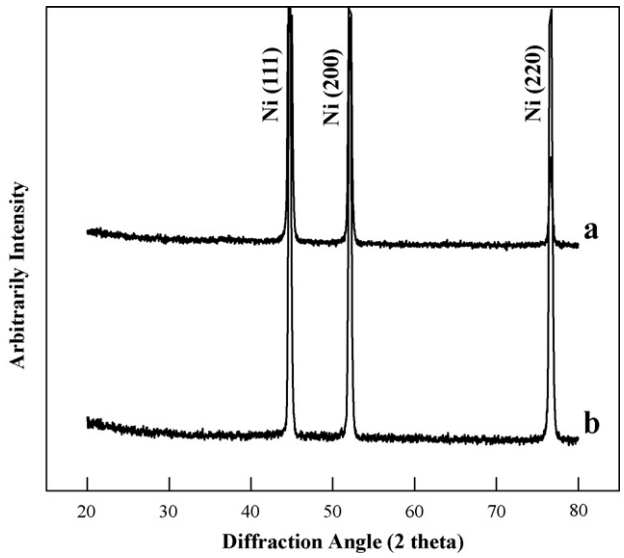

Fig. 3. GAXRD patterns of the as-deposited Mn (curve a) and Mn oxide–P (curve b) electrodes.

it was confirmed that the Mn oxide–P had the highest valence of Mn while the Mn oxide–CV had the lowest one. This trend was consistent with that recognized in the EDS analyses. However, it was found that the Mn valent state determined by XPS was higher than that estimated from EDS. Considering the different analytic depth of these two techniques, it may imply that the underneath part of the metallic Mn film was not completely oxidized. This hypothesis can be well supported by the fact that the total anodic charge (0.1 C cm^2) to oxidize the Mn film was less than that (0.3 C cm^2) to electrodeposit it, although this phenomenon was also partially attributed to the non-electrochemical oxidation of the Mn film as exposed to air. Fig. 4(b) shows the O 1s XPS spectra of the various Mn oxides. As revealed in this figure, each spectrum can be deconvoluted into three constituents that correspond to different oxygen-containing species such as anhydrous Mn oxide at 529.8 eV, Mn hydroxide at 531.2 eV, and structure water at 532.4 eV [26,27]. Clearly, the peak area (corresponded to the amount) of the different components for the Mn oxides significantly varied with their anodization history. The Mn oxide–P has the highest amount of the anhydrous compound among the electrodes. However, both the hydroxide and structure water contents would remarkably increase when the CV anodization method was employed.

Electrochemical performances of the Mn oxides prepared by the different anodization methods were evaluated by cyclic voltammetry (CV). Fig. 5 shows the voltammograms of the various electrodes, measured in 0.1 M Na_2SO_4 electrolyte at 25 °C, with a potential scan rate of 25 mV s^{-1}. As demonstrated, all the CV curves are essentially close to rectangular shapes, i.e. the respondent current does not really change within the potential window of 0–0.9 V but immediately switch its flowing direction as the potential is scanned reversely. Moreover, their mirror-image characteristics which show the approximate anodic and cathodic enclosed area can also be clearly recognized in this figure, revealing the ideal pseudocapacitive behavior of the oxide electrodes. It was noted that the working electrolyte (0.1 M Na_2SO_4 solution) can be the same with that used to oxidize the Mn films. The fact, from the viewpoint of practical applications, would simplify the process of fabricating a supercapacitor device. In addition, Fig. 5 indicates that the enclosed areas of the CV curves that correspond to energy storage capability of the oxide electrodes depend on their anodization conditions. Clearly, the Mn oxide–CV reveals the most promising performance among the electrodes. To quantitatively express the charge storage capacity, the specific capacitance (*C*) of the oxide

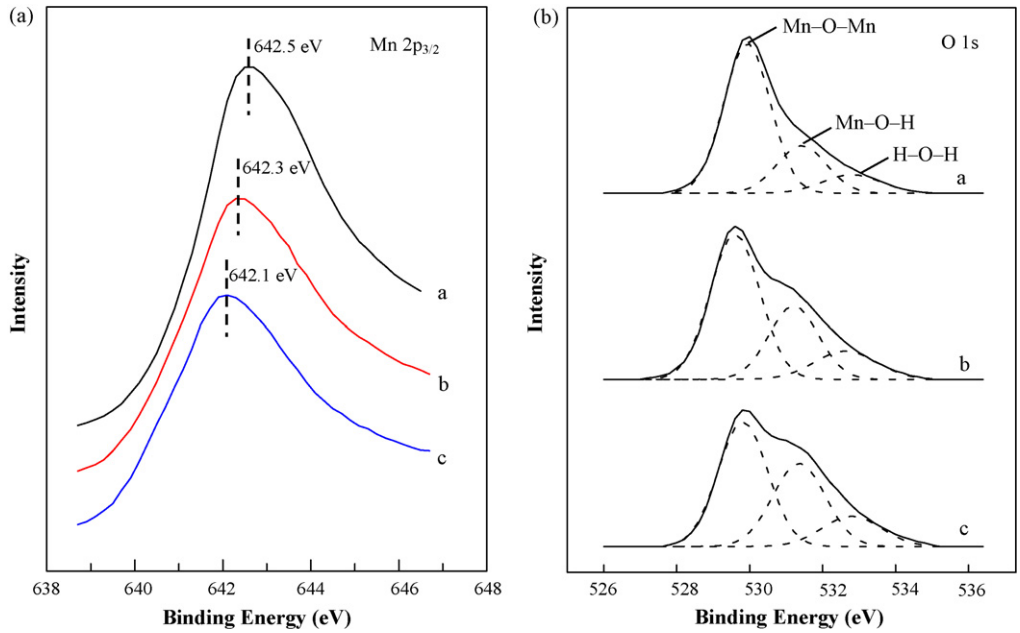

Fig. 4. (a) Mn $2p_{3/2}$ XPS spectra and (b) O 1s XPS spectra of the Mn oxide–P (curve a), Mn oxide–G (curve b), and Mn oxide–CV (curve c) electrodes.

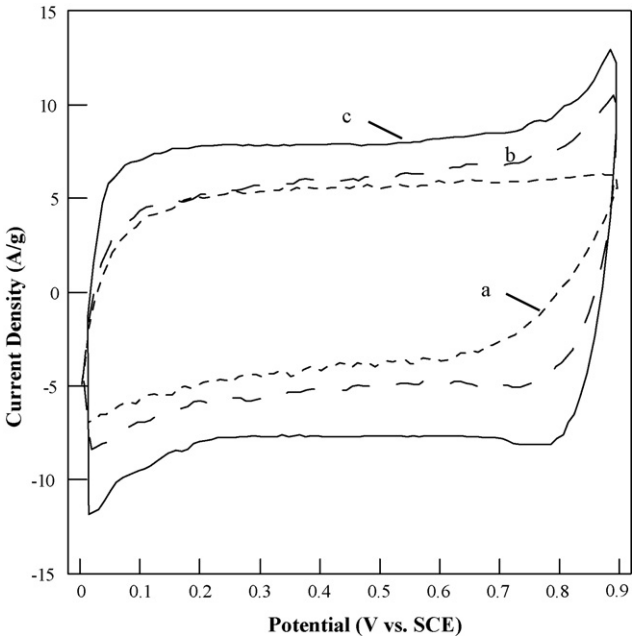

Fig. 5. Cyclic voltammograms of the Mn oxide–P (curve a), Mn oxide–G (curve b), and Mn oxide–CV (curve c) electrodes. They were measured in 0.1 M Na_2SO_4 electrolyte at 25 °C with a potential scan rate of 25 mV s^{-1}.

can be calculated according to the following equation:

$$C = \frac{\text{specific voltammetric charge}}{\text{potential range}} \quad (1)$$

where the specific voltammetric charge (voltammetric charge per gram of the oxide) was integrated from positive to negative sweeps of the CV curve. Fig. 6 summarizes the specific capacitances of the various Mn oxides measured at different CV scan rates, ranging from 5 mV s^{-1} to 150 mV s^{-1}. The optimum specific capacitance explored in this study is as high as 402 F g^{-1}, which is higher than many of the data that have been reported. This satisfactory value has indicated that the convenient electrochemical process proposed in this study is quite promising to fabricate the Mn oxide with great pseudocapacitive performance. The exceptional capacitance could be associated with the nanostructure of the initial Mn film, which was believed to be partially oxidized and remind intact in the underneath layer. The nanostructured Mn underlayer with large surface area actually acted as a supporter or current collector and consequently improved the utilization of the Mn oxide. In addition, the metallic and highly porous characteristics of the Mn supporter would increase both the electronic and ionic conductivity of the electrode. Therefore, the excellent electrochemical performance can be obtained. It is recognized in Fig. 6 that the anodization conditions significantly affect the specific capacitances of the prepared Mn oxides. The superior performance of the Mn oxide–CV electrode can be attributed to three major factors. (1) High surface area: As seen in Fig. 2, the Mn oxide–CV electrode is much more porous; therefore, the reactivity (or utilization) of the oxide can be enhanced. (2) Highly hydrous state: Since it has been known [8,28,29] that increasing the hydrous state can promote the ionic conductivity of the oxide, the high hydroxide and structure water contents of the Mn oxide–CV electrode (as shown in Fig. 4(b)) would be favorable for the great pseudocapacitive property. (3) Low Mn valent state: Our previous report [14] indicated that the lower (initial) Mn valent state was beneficial for specific capacitance of the oxide; this fact was probably because of the larger oxidation state change could be achieved during the charge–discharge process [16]. Fig. 6 also demonstrates that the specific capacitances of the electrodes decrease with increasing the potential scan rate; it is due to the kinetic limitation of the faradic redox reactions of the oxides. At a rate of 150 mV s^{-1}, the Mn oxide–P, Mn oxide–G, and Mn oxide–CV electrodes respectively possess 50%, 59%, and 70% of their specific capacitances measured at 5 mV s^{-1}. The great high-rate capability of the Mn oxide–CV electrode has made its superior capacitance even more pronounced at a high potential scan rate condition.

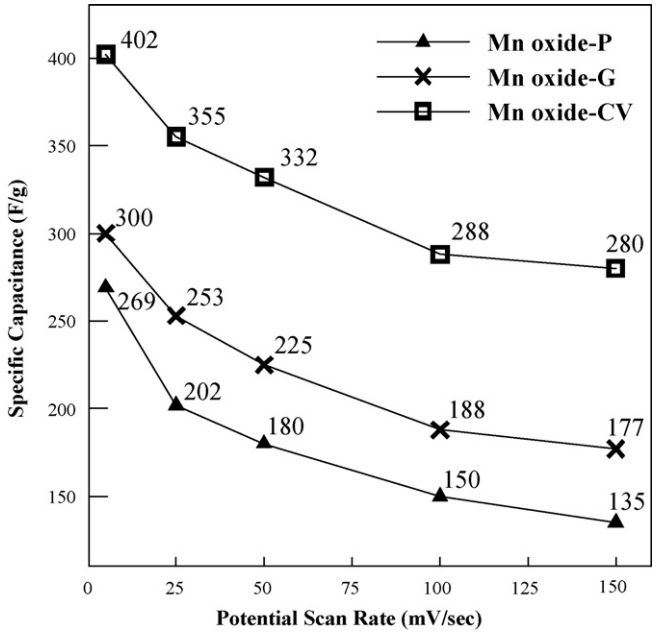

Fig. 6. The specific capacitances of the three different Mn oxide electrodes as a function of the potential scan rate during CV testing.

Electrochemical stability of the Mn oxides was evaluated by repeating the CV test for 500 cycles. The experimental data indicated that capacitance retained ratios (capacitance at the 500th cycle/capacitance at the first cycle) of the Mn oxide–P, Mn oxide–G, and Mn oxide–CV electrodes were 83%, 86%, and 94%, respectively. It was interesting to find that the cyclic stability of the Mn oxides also depended on their anodization history. Although the detailed mechanism that caused such difference in the capacitance fading rate was not clear yet, the phenomenon is conspicuous. According to the results presented in this paper, the Mn oxide–CV electrode which has high specific capacitance, good high-rate capability, and long cycle life is undoubtedly a very promising electrode material for using in supercapacitors.

4. Conclusions

The metallic, amorphous, and nanostructured characteristics of the Mn thin film electrodeposited in BMP–NTf_2 ionic liq-

uid have been considered to be unique for fabricating the Mn oxide with exceptional pseudocapacitive performance. It was also found that the Mn films could be anodized in Na_2SO_4 aqueous solution by the various electrochemical methods and transformed to the Mn oxides with different material characteristics. The Mn oxide anodized by the CV condition which had the largest surface area, highest hydrous state, and lowest Mn valent state showed the most promising specific capacitance of $402\,F\,g^{-1}$ among the electrodes. This oxide electrode also showed a great high-rate charge–discharge capability; moreover, its capacitance retained ratio after 500 CV scans was as high as 94%.

Acknowledgements

The authors would like to thank the National Science Council of the Republic of China for financially supporting this research under Contract No. NSC 95–2221–E–006–192.

References

[1] R. Kötz, M. Carlen, Electrochim. Acta 45 (2000) 2483–2498.
[2] H.Y. Lee, J.B. Goodenough, J. Solid State Chem. 144 (1999) 220–223.
[3] S.C. Pang, M.A. Anderson, T.W. Chapman, J. Electrochem. Soc. 147 (2000) 444–450.
[4] M. Toupin, T. Brousse, D. Bélanger, Chem. Mater. 16 (2004) 3184–3190.
[5] H.Y. Lee, V. Manivannan, J.B. Goodenough, Comptes Rendus Chimie 2 (1999) 565–577.
[6] S. Bach, J.P. Pereira-Ramos, N. Baffier, J. Solid State Chem. 120 (1995) 70–73.
[7] M. Toupin, T. Brousse, D. Bélanger, Chem. Mater. 14 (2002) 3946–3952.
[8] H. Kim, N. Branko, Popov, J. Electrochem. Soc. 150 (2003) D56–D62.
[9] Y.U. Jeong, A. Manthiram, J. Electrochem. Soc. 149 (2002) A1419–A1422.
[10] R.N. Reddy, R.G. Reddy, J. Power Sources 124 (2003) 330–337.
[11] J.N. Broughton, M.J. Brett, Electrochem. Solid State Lett. 5 (2002) A279–A282.
[12] V. Subramanian, H. Zhu, R. Vajtai, P.M. Ajayan, B. Wei, J. Phys. Chem. B 109 (2005) 20207–20214.
[13] C.C. Hu, T.W. Tsou, Electrochem. Commun. 4 (2002) 105–109.
[14] J.K. Chang, W.T. Tsai, J. Electrochem. Soc. 150 (2003) A1333–A1338.
[15] S. Wen, J.W. Lee, I.H. Yeo, J. Park, S.I. Mho, Electrochim. Acta 50 (2004) 849–855.
[16] J.K. Chang, M.T. Lee, W.T. Tsai, J. Power Sources 166 (2007) 590–594.
[17] H.Y. Lee, S.W. Kim, H.Y. Lee, Electrochem. Solid State Lett. 4 (2001) A19–A22.
[18] J.K. Chang, W.T. Tsai, J. Appl. Electrochem. 34 (2004) 953–961.
[19] J.K. Chang, C.T. Lin, W.T. Tsai, Electrochem. Comm. 6 (2004) 666–671.
[20] J.K. Chang, Y.L. Chen, W.T. Tsai, J. Power Sources 135 (2004) 344–353.
[21] J.K. Chang, W.T. Tsai, J. Electrochem. Soc. 152 (2005) A2063–A2068.
[22] D.R. MacFarlane, P. Meakin, J. Sun, N. Amini, M. Forsyth, J. Phys. Chem. B 103 (1999) 4164–4170.
[23] J.K. Chang, W.T. Tsai, P.Y. Chen, C.H. Huang, F.H. Yeh, I.W. Sun, Electrochem. Solid State Lett. 10 (2007) A9–A12.
[24] B.R. Strohmeier, D.M. Hercules, J. Phys. Chem. 88 (1984) 4922–4929.
[25] B.N. Ivanov-Emin, N.A. Nevskaya, B.E. Zaitsev, T.M. Ivanova, Zh. Neorg. Khim. 27 (1982) 3101–3104.
[26] M. Chigane, M. Ishikawa, J. Electrochem. Soc. 147 (2000) 2246–2251.
[27] M. Chigane, M. Ishikawa, M. Izaki, J. Electrochem. Soc. 148 (2001) D96–D101.
[28] S.B. Kanungo, K.M. Parida, B.R. Sant, Electrochim. Acta 26 (1981) 1147–1156.
[29] D.A. Mckeown, P.L. Hagans, L.P.L. Carette, A.E. Russell, K.E. Swider, D.R. Rolison, J. Phys. Chem. B 103 (1999) 4825–4832.